Frequency comb-based time transfer over a 159 km long installed fiber network

M. Lessing,[1,2] H. S. Margolis,[1] C. T. A. Brown,[2] and G. Marra[1,a)]

[1)] *National Physical Laboratory, Hampton Road, Teddington, Middlesex, TW11 0LW, UK*

[2)] *SUPA, School of Physics and Astronomy, University of St Andrews, St Andrews, Fife, KY16 9SS, UK*

(Dated: 12 May 2017)

We demonstrate a frequency comb-based time transfer technique on a 159 km long installed fiber link. Timing information is superimposed onto the optical pulse train of an ITU-channel-filtered mode-locked laser using an intensity modulation scheme. The environmentally induced optical path length fluctuations are compensated using a round-trip phase noise cancellation technique. When the fiber link is stabilized a time deviation of 300 fs at 5 s and an accuracy at the 100 ps level is achieved.

PACS numbers: 06

Driven by improvements in the performance of optical atomic clocks, which can now achieve accuracies and stabilities at the 10^{-18} level[1–3], much research has been undertaken in the field of frequency transfer via fiber networks to overcome the limitations of satellite-based techniques. It has been shown that the performance of fiber-based optical frequency transfer techniques is suitable for the comparison of state-of-the-art optical clocks on a continental scale[4–6]. Fiber-based time transfer techniques have also been shown to offer superior performance compared to their satellite-based counterparts. Accuracies of tens of ps have been reported for fiber lengths of hundreds of km[7,8] which is significantly better than that offered by routinely-used satellite-based two-way time transfer techniques (accuracy at the 1 ns level[9]). These fiber-based techniques could therefore be beneficial for clock comparisons for the computation of International Atomic Time. Several different fiber-based time transfer techniques have been investigated[7,8,10–14].

While there has been a demonstration of two-way time transfer over a 12 km free-space distance with fs level time deviation using optical frequency combs[15,16], all time transfer methods over longer fiber networks to date have been carried out using amplitude-modulated continuous wave (CW) lasers. In previous work, we have demonstrated microwave and optical frequency transfer on a 7 km long fiber link at a level better than 1×10^{-17} by propagation of a 30 nm-wide optical frequency comb[17]. Here, we demonstrate time transfer over a 159 km long installed fiber network using an ITU-channel-filtered mode-locked laser (MLL). This opens the way for transferring microwave frequencies, optical frequencies and time simultaneously via fiber networks using optical frequency combs.

The dark fiber network used for this experiment consists of two parallel 79.6 km long fiber links between the National Physical Laboratory (NPL) and Reading. In order to operate in the typical configuration for testing time and frequency transfer methods, in which the user and transmitter end of the experiment are co-located in the same laboratory, the two parallel fibers are joined in Reading to form a loop.

The experimental set-up can be seen in figure 1. Initially we measured the transfer stability using the setup depicted in the grayed out areas[18]. We then implemented some minor changes to improve reliability and minimize reflections and we measured the transfer accuracy with this latter setup. An ITU-channel-filtered mode-locked laser (M-Comb, Menlo Systems) with a repetition rate of 100 MHz is used for the time transfer experiments. The repetition rate of the MLL is locked to a signal derived from a hydrogen maser, but the carrier-envelope offset frequency is not stabilized. The ITU channel used in this experiment is channel 44, centred around 1542.14 nm. Filtering to a single ITU channel (100 GHz) reduces the number of optical modes to several hundred corresponding to a pulse width of a few ps for Fourier-limited pulses. A total of eleven channel 44 filters were employed; one after the unidirectional EDFA, and one on either side of each bidirectional EDFA in order to reduce spontaneous emission noise and avoid lasing effects.

Three dispersion compensation modules are employed to compensate for a total of approximately 198 km of single-mode fibre (SMF-28). Fibre spools are added to the installed fiber link (159.2 km) to achieve this overall length. The residual pulse broadening is estimated to be only around two ps. The overall one-way loss of the fiber link including all components is approximately 80 dB whilst the combined gain of the five bidirectional EDFAs (bi-EDFA) is approximately 100 dB. The input power of the first bi-EDFA was set to -25dBm to maximize the ratio between reflections and useful returned signals on port 3. A signal of around -5 dBm was incident on the photodiode at the user end.

In order to cancel the environmentally-induced optical path length fluctuations of the fibre link, a round-trip phase noise cancellation technique is employed based

[a)] Electronic mail: giuseppe.marra@npl.co.uk

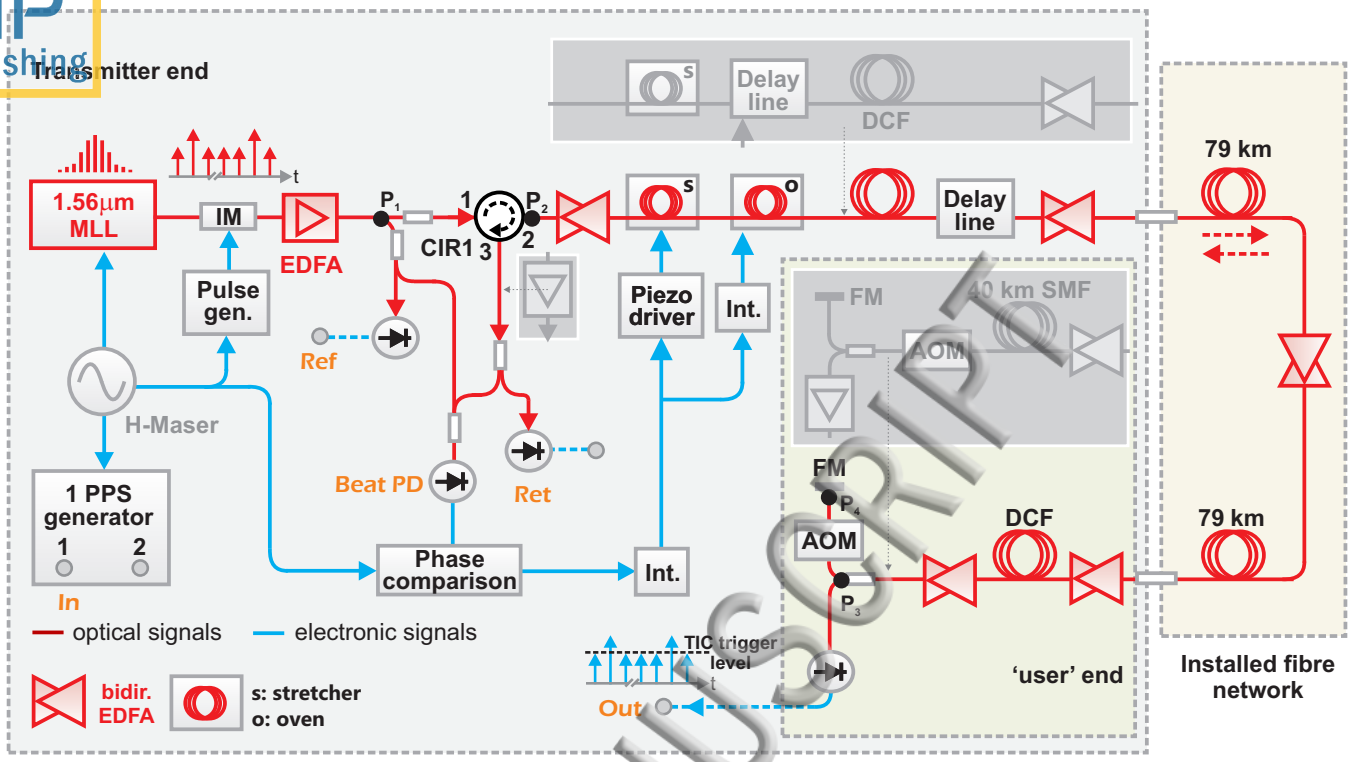

FIG. 1. Schematic of the experimental set-up. The phase fluctuations of the fiber link are measured by comparing the optical modes of the local laser with those of the returned laser and suppressed using two fiber stretchers and a temperature-controlled fiber spool. The time transfer performance is characterised by measuring the time intervals using the time marker pulses and an SR620 time interval counter. PD: photodiode; IM: intensity modulator; Pulse gen.: pulse generator; Int.: integrator; EDFA: erbium-doped fiber amplifier; CIR: circulator; det.: photodetector; MLL: mode-locked laser; DCF: dispersion compensating fiber; FM: Faraday mirror; bidir.: bidirectional; PPS: pulse per second; TIC: time interval counter; AOM: acousto optical modulator. Pulse amplification following the photodiodes not shown in this diagram.

on the detection of the optical phase difference between two combs[17,19,20]. The optical beat from which the error signal is derived is generated from the optical modes of the local comb and the returned comb, which has been frequency-shifted by 154 MHz due to double-passing an AOM at the user end. In order to achieve temporal overlap between the two pulse trains at the Beat PD, short fiber patch cords and an optical delay line are used. The fiber link is stabilized employing a fast and a slow feedback loop. The fast feedback loop (bandwidth of approximately 200 Hz) controls two fibre stretchers (OptiPhase) with a delay range of 100 ps. The slow feedback loop (time constant of 10^4 s) employs a temperature-controlled, 12.5 km long fibre spool with a delay range of approximately 13 ns. Whilst the carrier-envelope offset frequency of the mode-locked laser is not stabilized, as no detection stage is present in the system used for this experiment, fluctuations at time scales much larger than the propagation round trip time are greatly suppressed as they are common-mode between the reference and returned pulse trains.

In order to superimpose timing information onto the optical pulse train, an amplitude modulation scheme is used in which time marker pulses have an amplitude 1.7 times higher than to other pulses. The time marker pulses are used to measure the time delay of the fiber link, while the pulses with smaller amplitude are employed in the phase noise cancellation technique. In order to achieve the amplitude modulation, a 10 GHz Mach-Zehnder intensity modulator (MZIM; LN81S-FC, Thorlabs) is driven by a commercial pulse generator (Agilent 81101A) with a bandwidth of 50 MHz, locked to the hydrogen maser. The generator produces pulses of 10 ns length and an amplitude of 2 V, with rising and falling edges 2.5 ns long. The timing instability of the pulse generator has negligible effect on the time transfer stability as the timing information is embedded in the optical pulse train rather than in its amplitude modulation and the modulation is used only to select the marker pulse. A feedback loop stabilizes the MZIM to the positive quadrature point in order to avoid temperature-induced amplitude fluctuations of the marker pulses that would translate into timing errors of the transferred pulse train. Modulation sidebands at an offset frequency corresponding to the inverse of the marker pulse repetition rate (800 µs in our experiment, leading to sidebands at

(1.25 kHz) will be generated on the harmonics of the MLL repetition rate detected by the local and remote photodiodes. However, as only one out of every several tens of thousands pulses is modulated (80,000 in our experiment), their magnitude is extremely small. Should this level be still too high for ultra-low noise applications, it would be possible to reduce the modulation index (until proper detection of the marker pulse is no longer possible), further increase the interval between the marker pulses and/or phase lock a good quality local oscillator to the transferred signal with a bandwidth smaller than the inverse of the interval between time marker pulses.

The procedure used to calibrate the time transfer set-up is based on the same concept as in the work described by Krehlik et al.[7] and a timing model of the set-up is shown in figure 2. The absolute time delay between the local time reference (1 PPS generator) and the corresponding time marker pulse at the user end is calculated as half of the measured round-trip delay, which can be monitored at the transmitter end, plus a constant calibration factor which takes account of any delays which are non-common to the forward and backward directions of the fiber link. The reference output and the return output of the set-up are used to measure the round-trip delay. The calibration factor has to be determined before the time transfer experiment is carried out. The non-common delays t_2, t_3, t_5, t_6 and t_7 experienced by the time marker pulses (due to fibre and electrical components) are defined by the points P_1, P_2, P_3, and P_4 shown in figure 1 and figure 2. Since the pulse generator superimposes timing information onto the optical pulse train rather than the PPS generator (PPS-2 SpectraDynamics), there is a time interval $\tau_{\mathrm{In}\to\mathrm{Ref}}$ between the release of the 1 PPS signal and the arrival of the corresponding optical time marker pulse at the reference output which has to be determined. This time interval can be measured at the transmitter end by comparing the delay between the PPS signal and the time marker pulse at the reference output, and it will be constant during operation of the time transfer link as the MLL, the pulse generator and the PPS generator are all locked to the hydrogen maser. The time interval $\tau_{\mathrm{In}\to\mathrm{Ref}}$ can be expressed as the sum of the following time delays experienced by the time marker pulse: t_x, which is the sum of the time it takes the marker pulse to travel from the unknown point where it is when the PPS signal is released to P_1, and t_2. We denote by $\tau_{\mathrm{In}\to\mathrm{Out}}$ the time interval between the output pulse at the PPS generator and the electrical pulse detected by the photodetector at the user end (Out), by $\tau_{\mathrm{Ref}\to\mathrm{Out}}$ the time interval between the pulses detected by the reference (Ref) and user (Out) photodetectors and by $\tau_{\mathrm{Ref}\to\mathrm{Ret}}$ the time interval between the pulse detected by the reference (Ref) and the return photodetectors (Ret) after the pulse train has travelled a round trip through the 79.6 km-long optical link. In all cases the detected pulses are amplified to a suitable amplitude (typically 1.5 V) for counting using RF amplifiers and the amplitude was matched, using a manually variable optical attenuator, by visualizing the signal on a fast oscilloscope.

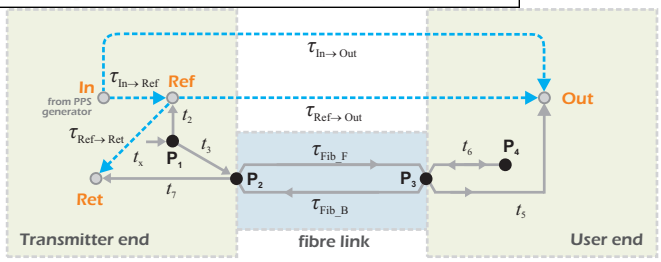

FIG. 2. Timing model of the time transfer set-up.

These time intervals (dashed blue lines in figure 2) can be expressed as:

$$\tau_{\mathrm{In}\to\mathrm{Ref}} = t_x + t_2, \tag{1}$$

$$\tau_{\mathrm{In}\to\mathrm{Out}} = t_x + t_3 + \tau_{\mathrm{Fib\_F}} + t_5, \tag{2}$$

$$\tau_{\mathrm{Ref}\to\mathrm{Out}} = -t_2 + t_3 + \tau_{\mathrm{Fib\_F}} + t_5, \tag{3}$$

$$\tau_{\mathrm{Ref}\to\mathrm{Ret}} = -t_2 + t_3 + \tau_{\mathrm{Fib\_F}} + 2t_6 + \tau_{\mathrm{Fib\_B}} + t_7, \tag{4}$$

where $\tau_{\mathrm{Fib\_F}}$ and $\tau_{\mathrm{Fib\_B}}$ are the delays of the forward and the backward directions of the fiber link. Here, there is no difference between $\tau_{\mathrm{Fib\_F}}$ and $\tau_{\mathrm{Fib\_B}}$ due to the Sagnac effect, since the transmitter end and user end of the set-up are located in the same laboratory. A small difference between $\tau_{\mathrm{Fib\_F}}$ and $\tau_{\mathrm{Fib\_B}}$ may arise due to polarisation mode dispersion (see table I). Using equations 1–4, the delay between the local time reference signal (PPS generator) and the user timing signal (time marker pulse) can be expressed as:

$$\tau_{\mathrm{In}\to\mathrm{Out}} = \tau_{\mathrm{In}\to\mathrm{Ref}} + \frac{1}{2}\tau_{\mathrm{Ref}\to\mathrm{Ret}} + \frac{1}{2}(\tau_{\mathrm{Fib\_F}} - \tau_{\mathrm{Fib\_B}}) + \frac{1}{2}\tau_{\mathrm{c}}, \tag{5}$$

where τ_{c} is a calibration factor that takes account of the non-common paths between the forward and the backward directions of the path of the time marker pulses:

$$\tau_{\mathrm{c}} = -t_2 + t_3 + 2t_5 - 2t_6 - t_7. \tag{6}$$

In order to determine the calibration factor τ_{c}, the local and the remote modules must be located in the same laboratory. The fiber link is replaced by a variable fiber attenuator which is tuned to give the same attenuation as the fiber link. As a consequence, the difference between $\tau_{\mathrm{Fib\_F}}$ and $\tau_{\mathrm{Fib\_B}}$ is negligible and (inserting equations 1, 2 and 4 into equation 5) the calibration factor is given by:

$$\tau_{\mathrm{c}} = 2\tau'_{\mathrm{Ref}\to\mathrm{Out}} - \tau'_{\mathrm{Ref}\to\mathrm{Ret}}, \tag{7}$$

where the primes indicate that this is the calibration measurement. Hence, τ_{c} can be determined by measuring only two time delays. Once the calibration factor is

Source	Uncertainty (ps)	Sensitivity coefficient	Uncertainty contribution (ps)
$\tau_{\mathrm{In}\to\mathrm{Ref}}$	50	1	50
$\tau_{\mathrm{Ref}\to\mathrm{Ret}}$	50	0.5	25
PMD	0.6	0.5	0.3
τ_c	112	0.5	56
Total uncertainty $\tau_{\mathrm{In}\to\mathrm{Out}}$			**80 ps**

TABLE I. Uncertainty budget for determining $\tau_{\mathrm{In}\to\mathrm{Out}}$ using an SR620 time interval counter. The sensitivity factors from equation 5 are taken into consideration. The uncertainty of τ_c is obtained by adding the contributions of the right side of equation 7 in quadrature. PMD: Polarisation mode dispersion.

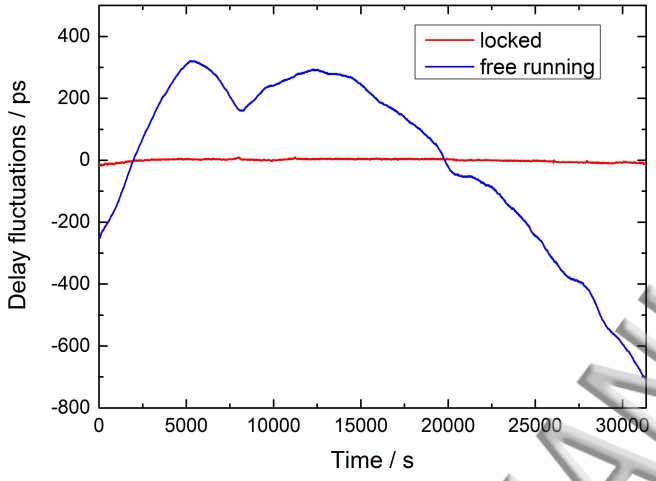

FIG. 3. Residual delay fluctuations of the fiber link for the free-running case (blue line) and the locked case (red line).

known, the absolute delay $\tau_{\mathrm{In}\to\mathrm{Out}}$ of any delay-stabilized fiber link can be determined via equation 5 by measuring $\tau_{\mathrm{In}\to\mathrm{Ref}}$ and $\tau_{\mathrm{Ref}\to\mathrm{Ret}}$ at the transmitter end. Here, the time delays are measured using an SR620 (Stanford Research Systems) time interval counter which has an uncertainty for relative time interval measurements of approximately 50 ps. The total uncertainty for determining $\tau_{\mathrm{In}\to\mathrm{Out}}$ (80 ps, see table I) is obtained by adding all uncertainty contributions of the terms on the right side of equation 5 in quadrature.

The time transfer stability is determined by measuring the time interval between the points Ref and Out of figure 1 using the SR620 time interval counter triggered by the time marker pulses (period 800 µs) and averaging over 1000 samples. The trigger level was set to 80% of the marker pulse amplitude. The residual delay fluctuations and the corresponding time deviation of the free running (blue traces) and the stabilized fiber link (red traces) can be seen in figure 3 and figure 4 respectively.

The stabilization of the fiber link results in a reduction of the time deviation by a factor of approximately 50 (at 5000 s) compared to the free running link. When the link is stabilized, the time deviation reaches a value of approximately 300 fs at 5 s. The time deviation at this

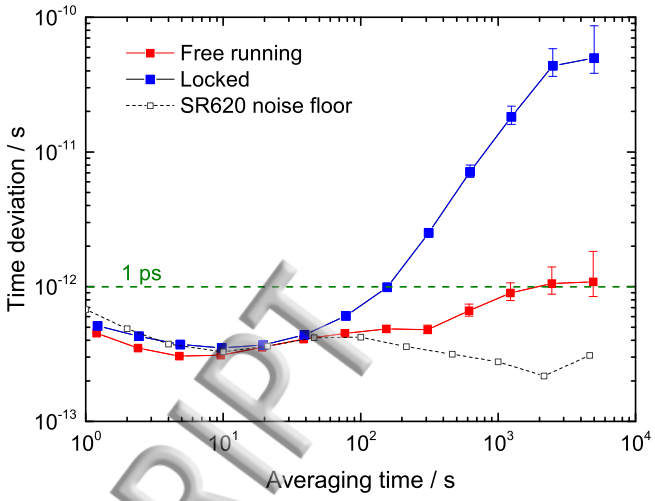

FIG. 4. Time deviation of the NPL–Reading fiber link calculated from the free-running (blue solid squares) and locked (solid red squares) delay fluctuations shown in figure 3. The measurement limit of the SR620 is also shown (black open squares).

Time interval measurements	
Signal	Time interval (ps)
Ref	163 266 631
Ret	163 564 361
Out	163 395 623
Calculated time delays	
Delay	Time interval (ps)
$\tau'_{\mathrm{Ref}\to\mathrm{Out}}$	128 992
$\tau'_{\mathrm{Ref}\to\mathrm{Ret}}$	297 730
$\tau_c = (-39.7 \pm 0.1)$ ns	

TABLE II. Results of a time transfer calibration measurement. The time delays of interest at the bottom of the table are calculated from the time interval measurements at the top of the table. In order to obtain relative time interval measurements, channel A of the time interval counter is triggered by the auxiliary channel 2 output of the PPS generator for all measurements while channel B is sequentially connected to the various signals of interest.

time scale is limited by the residual fluctuations of the SR620 time interval counter.

In order to verify the time transfer accuracy, a total of four calibration measurements (determination of τ_c) and six verification measurements (comparison between prediction and direct measurement of $\tau_{\mathrm{In}\to\mathrm{Out}}$) were carried out over the course of several days. The result from one calibration measurement can be seen in table II. The measured time intervals at the top of the table were obtained by measuring each time interval for approximately 5 minutes (using the SR620) and subsequently calculating the average value; this is the case in the verification measurements as well. All four calibration measurements were in agreement within their uncertainty of 112 ps; the average value was approximately $\tau_c = -39.8$ ns, the standard deviation was 60 ps and the peak-to-peak deviation

Signal	Time interval (ps)
Time interval measurements	
In	4 152
Ref	163 264 768
Ret	788 384 111
Out	475 804 491
Calculated time delays	
Delay	Time interval (ps)
$\tau_{\mathrm{In}\to\mathrm{Ref}}$	163 260 616
$\tau_{\mathrm{Ref}\to\mathrm{Out}}$	1 112 539 723
$\tau_{\mathrm{Ref}\to\mathrm{Ret}}$	2 225 119 343
$\boldsymbol{\tau_{\mathrm{In}\to\mathrm{Out}}}$ **(prediction)**	$(\mathbf{1\,275\,800.41 \pm 0.08})$ **ns**
$\boldsymbol{\tau_{\mathrm{In}\to\mathrm{Out}}}$ **(measurement)**	$(\mathbf{1\,275\,800.34 \pm 0.05})$ **ns**

TABLE III. Results of a time transfer verification measurement. The predicted value of the delay $\tau_{\mathrm{In}\to\mathrm{Out}}$ and the direct measurement of $\tau_{\mathrm{In}\to\mathrm{Out}}$ agree within their associated uncertainties.

was 131 ps.

For the verification measurements the optical path length of the fiber link was stabilized. The result from one verification measurement can be seen in table III. Since the one-way delay of the fiber link is approximately 1.1 ms and the time marker period was set to 800 µs, different time marker pulses start and stop the time interval measurement on the SR620. This has to be accounted for when calculating the time delays of interest in table III. To obtain the correct value for $\tau_{\mathrm{Ref}\to\mathrm{Out}}$ ($\tau_{\mathrm{Ref}\to\mathrm{Ret}}$), 800 µs (1.6 ms) have to be added to the difference between Out and Ref (Ret and Ref). The largest possible time marker repetition rate, that still enables any pulse ambiguity to be resolved in a simple way, was chosen for averaging purposes.

In five of the six verification measurements the direct measurement and the predicted value of $\tau_{\mathrm{In}\to\mathrm{Out}}$ were in agreement within their associated uncertainties. Only in one measurement was the difference (−144 ps) slightly larger than the combined one sigma uncertainties. The average deviation between the prediction and the direct measurement was −32 ps, the standard deviation was 104 ps.

In summary, a time transfer technique based on the propagation of an optical pulse train from a mode-locked laser was demonstrated over a 159 km-long installed fiber link. A time transfer stability of approximately 300 fs at 5 s was measured. This performance, which is limited by the residual fluctuations of the SR620 time interval counter, is at a similar level as the state-of-the-art performance reported by Krehlik et al.[7,21] using amplitude-modulated CW lasers. The time transfer accuracy has been measured to be at the 100 ps level. This performance was also limited by the SR620 time interval counter. In the future, the accuracy could be improved, potentially to 10 ps, by using a digital storage oscilloscope rather than a standard time interval counter. This experiment, in conjunction with our previous work[17], demonstrates that frequency comb-based fiber transfer techniques can be used to transfer time, microwave frequencies and optical frequencies simultaneously over long telecommunication fiber links with high stability and accuracy levels.

Funding. This work is supported by the UK National Measurement System and the European Metrology Research Programme (EMRP). The EMRP is jointly funded by the EMRP participating countries within EURAMET and the European Union. The fibre link used in this work is funded by the UK Space Agency. ML acknowledges support from the Engineering and Physical Sciences Research Council (EPSRC) through the Centre for Doctoral Training in Applied Photonics. Maurice Lessing is now at Menlo Systems GmbH, Am Klopferspitz 19a, 82152, Martinsried, Germany

[1] B. Bloom, T. Nicholson, J. Williams, S. Campbell, M. Bishof, X. Zhang, W. Zhang, S. Bromley, and J. Ye, Nature **506**, 71 (2014).
[2] T. Nicholson, S. Campbell, R. Hutson, G. Marti, B. Bloom, R. McNally, W. Zhang, M. Barrett, M. Safronova, and G. Strouse, Nature Communications **6**, 6896 (2015).
[3] I. Ushijima, M. Takamoto, M. Das, T. Ohkubo, and H. Katori, Nature Photonics **9**, 185 (2015).
[4] K. Predehl, G. Grosche, S. Raupach, S. Droste, O. Terra, J. Alnis, T. Legero, T. W. Hänsch, T. Udem, R. Holzwarth, and H. Schnatz, Science **336**, 441 (2012).
[5] S. Droste, F. Ozimek, T. Udem, K. Predehl, T. W. Hänsch, H. Schnatz, G. Grosche, and R. Holzwarth, Physical Review Letters **111**, 110801 (2013).
[6] D. Calonico, E. Bertacco, C. Calosso, C. Clivati, G. Costanzo, M. Frittelli, A. Godone, A. Mura, N. Poli, D. Sutyrin, G. Tino, M. E. Zucco, and F. Levi, Applied Physics B **117**, 979 (2014).
[7] P. Krehlik, Ł. Śliwczyński, Ł. Buczek, and M. Lipiński, IEEE Transactions on Instrumentation and Measurement **61**, 2844 (2012).
[8] Ł. Śliwczyński, P. Krehlik, A. Czubla, Ł. Buczek, and M. Lipiński, Metrologia **50**, 133 (2013).
[9] D. Piester, A. Bauch, L. Breakiron, D. Matsakis, B. Blanzano, and O. Koudelka, Metrologia **45**, 185 (2008).
[10] O. Lopez, A. Kanj, P.-E. Pottie, D. Rovera, J. Achkar, C. Chardonnet, A. Amy-Klein, and G. Santarelli, Applied Physics B **110**, 3 (2013).
[11] F. Yin, Z. Wu, Y. Dai, T. Ren, K. Xu, J. Lin, and G. Tang, Optics Letters **39**, 3054 (2014).
[12] M. Rost, D. Piester, W. Yang, T. Feldmann, T. Wübbena, and A. Bauch, Metrologia **49**, 772 (2012).
[13] B. Wang, C. Gao, W. Chen, J. Miao, X. Zhu, Y. Bai, J. Zhang, Y. Feng, T. Li, and L. Wang, Scientific Reports **2** (2012).
[14] S. M. Raupach and G. Grosche, IEEE Transactions on Ultrasonics, Ferroelectrics, and Frequency Control **61**, 920 (2014).
[15] F. R. Giorgetta, W. C. Swann, L. C. Sinclair, E. Baumann, I. Coddington, and N. R. Newbury, Nature Photonics **7**, 434 (2013).
[16] L. C. Sinclair, W. C. Swann, H. Bergeron, E. Baumann, M. Cermak, I. Coddington, J. D. Deschnes, F. R. Giorgetta, J. C. Juarez, I. Khader, K. G. Petrillo, K. T. Souza, M. L. Dennis, and N. R. Newbury, Applied Physics Letters **109**, 15, (2015).
[17] G. Marra, H. S. Margolis, and D. J. Richardson, Optics Express **20**, 1775 (2012).
[18] M. Lessing, H. S. Margolis, C. T. A. Brown, and G. Marra, Conference on Lasers and Electro-Optics (CLEO), **20**, 1775 (2015).
[19] Y.-F. Chen, J. Jiang, and D. J. Jones, Opt. Express **14**, 12134 (2006).
[20] S. M. Foreman, K. W. Holman, D. D. Hudson, D. J. Jones, and J. Ye, Review of Scientific Instruments **78**, 021101 (2007).
[21] P. Krehlik, Ł. Śliwczyński, Ł. Buczek, J. Kołodziej, and M. Lipiński, Metrologia **52**, 82 (2015).

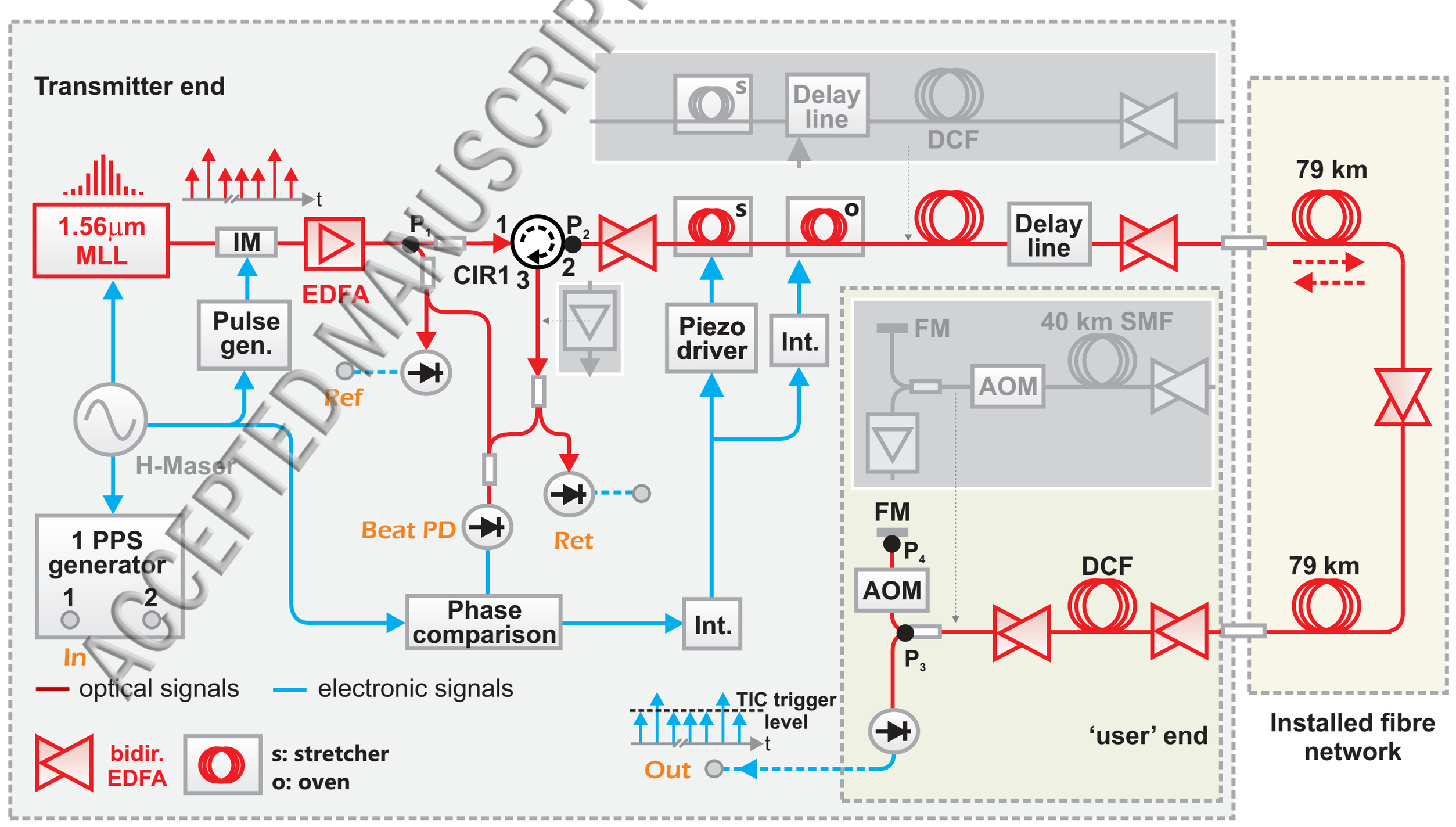

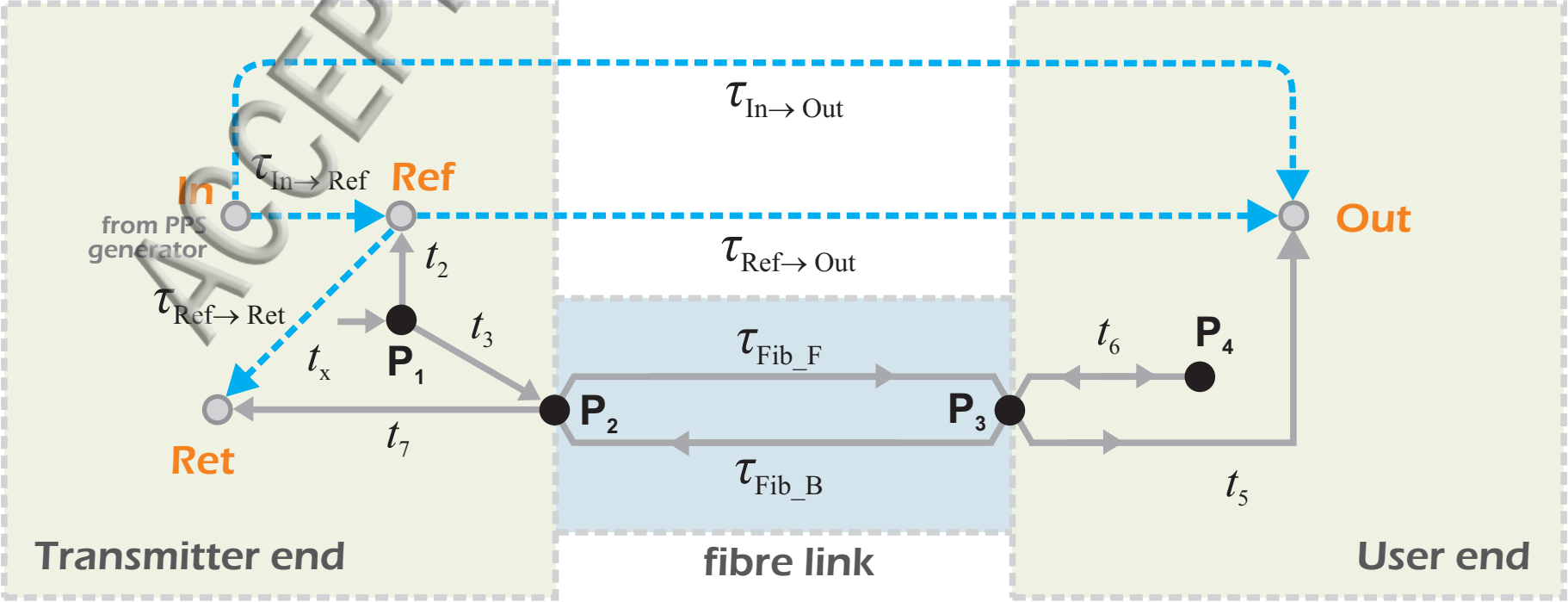
ACCEPTED
$\tau_{In\rightarrow Out}$
$\tau_{In\rightarrow Ref}$
In
Ref
from PPS generator
Out
$\tau_{Ref\rightarrow Out}$
t_2
$\tau_{Ref\rightarrow Ret}$
t_3
τ_{Fib_F}
t_6
P_4
t_x
P_1
P_2
P_3
t_7
Ret
τ_{Fib_B}
t_5
Transmitter end
fibre link
User end